ROSE-HULMAN INSTITUTE OF TECHNOLOGY

CHEMISTRY AND BIOCHEMISTRY

Case Studies in Viral Inhibition

(Yes, it does . . . No, it does NOT!)

Thymidine Kinase

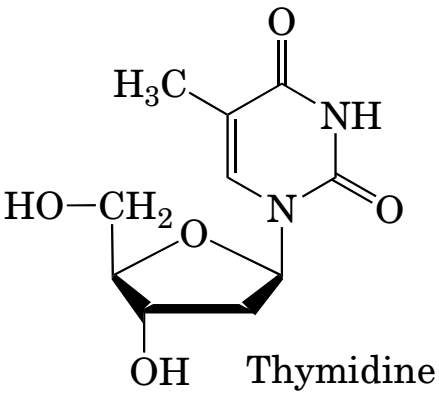

Thymidine

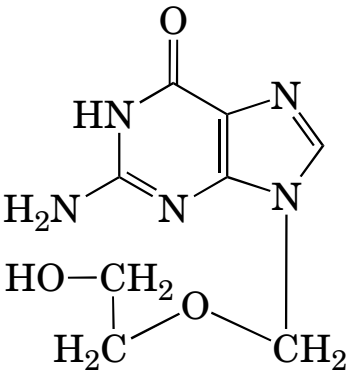

Acyclovir

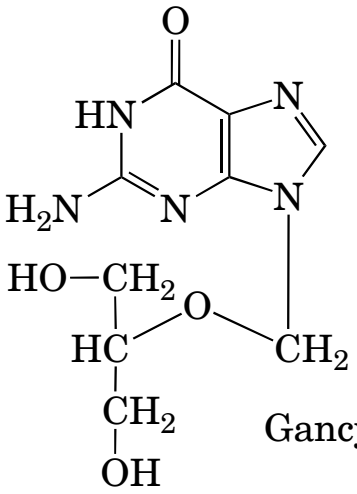

Gancyclovir

Influenza Replication

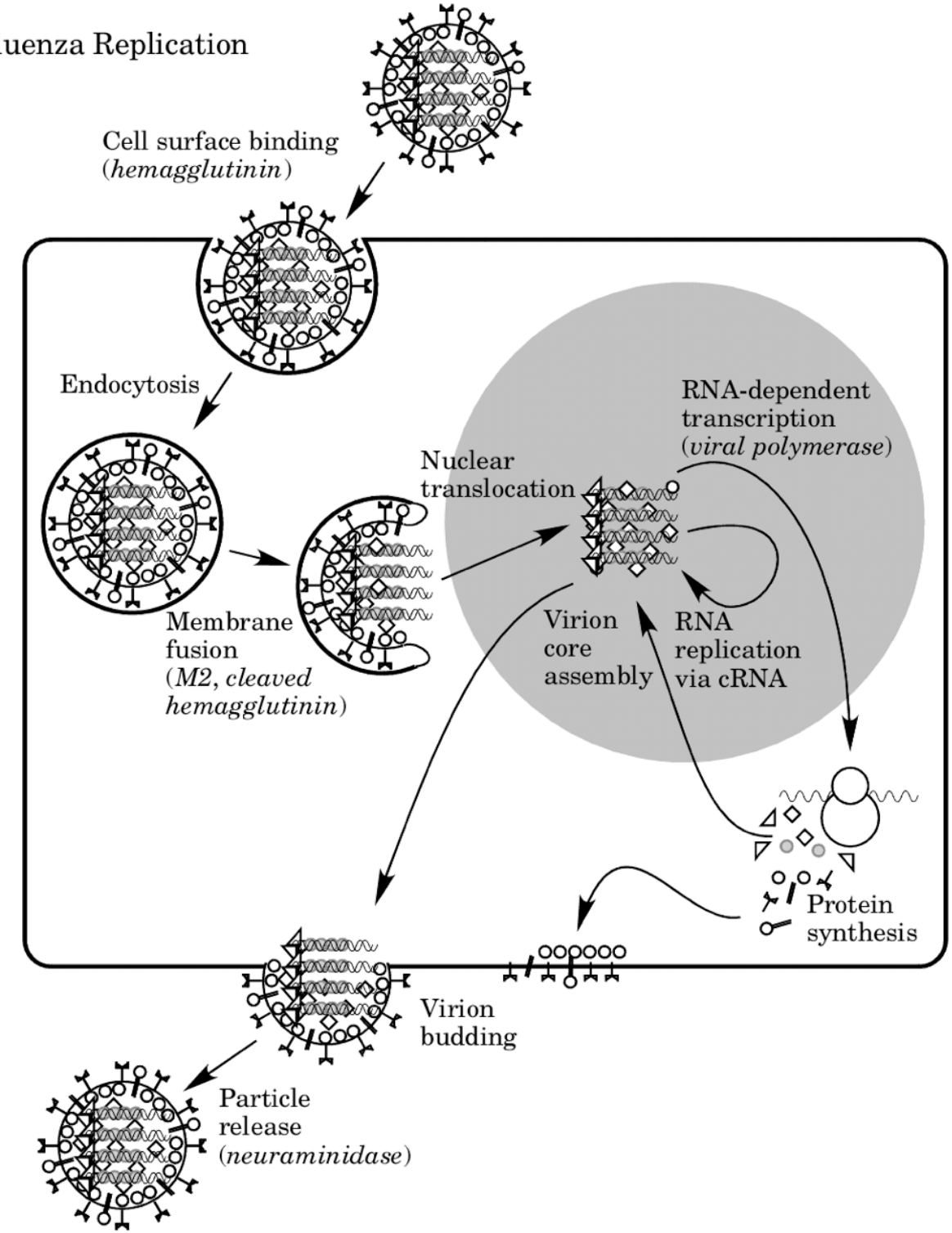

M2 Inhibitors

Amantadine

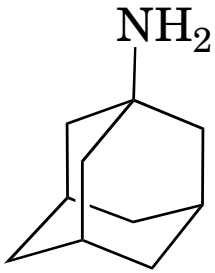

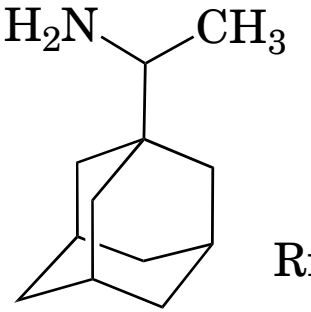

Rimantadine

M2 Structures

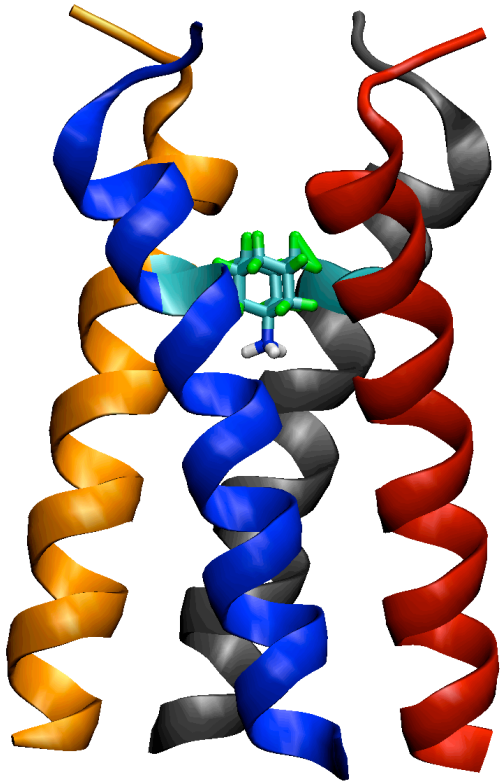

Cady *et al*.

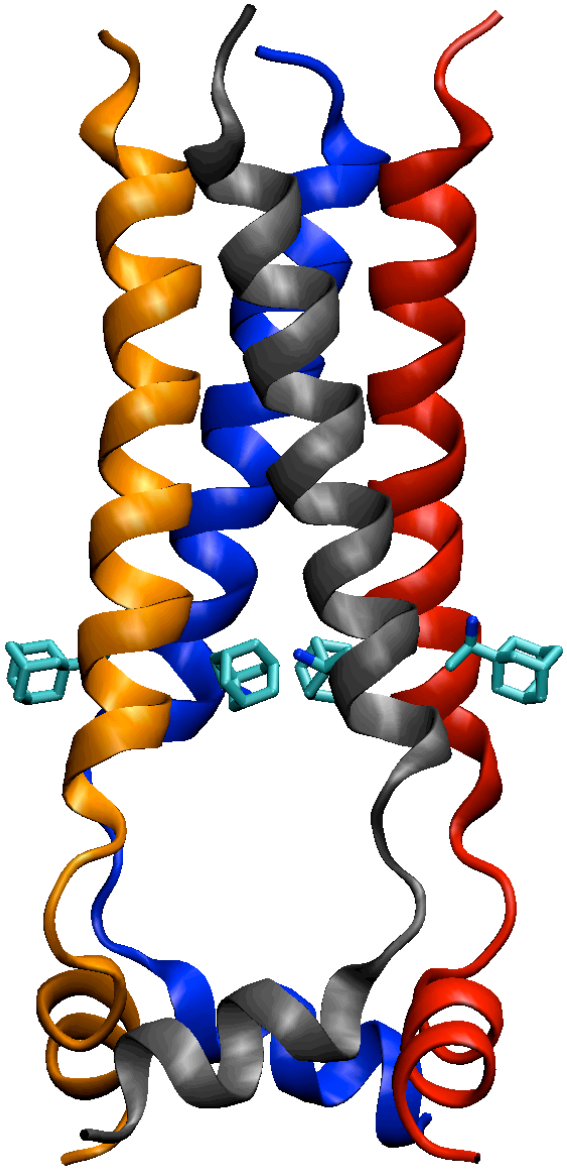

Schnell & Chou

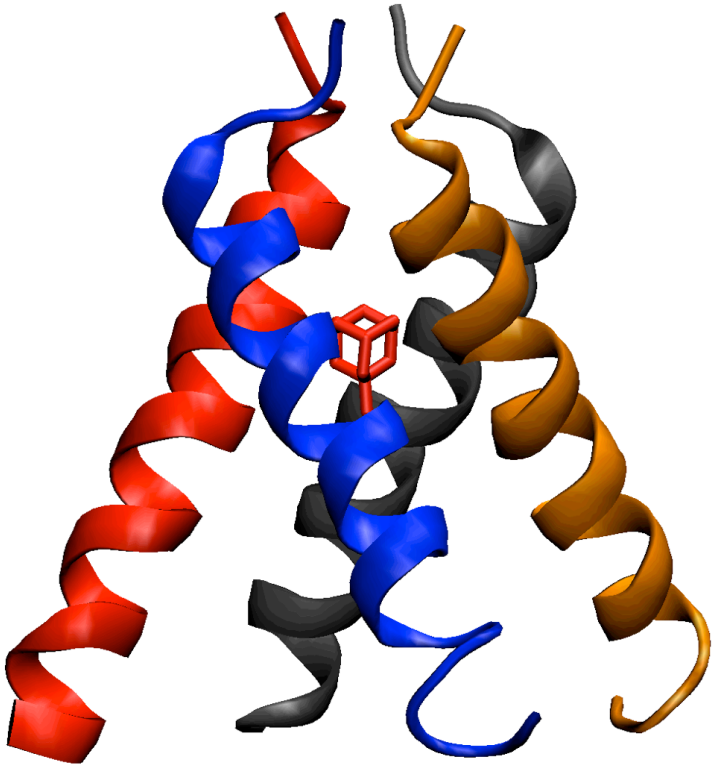

Stouffer *et al*.

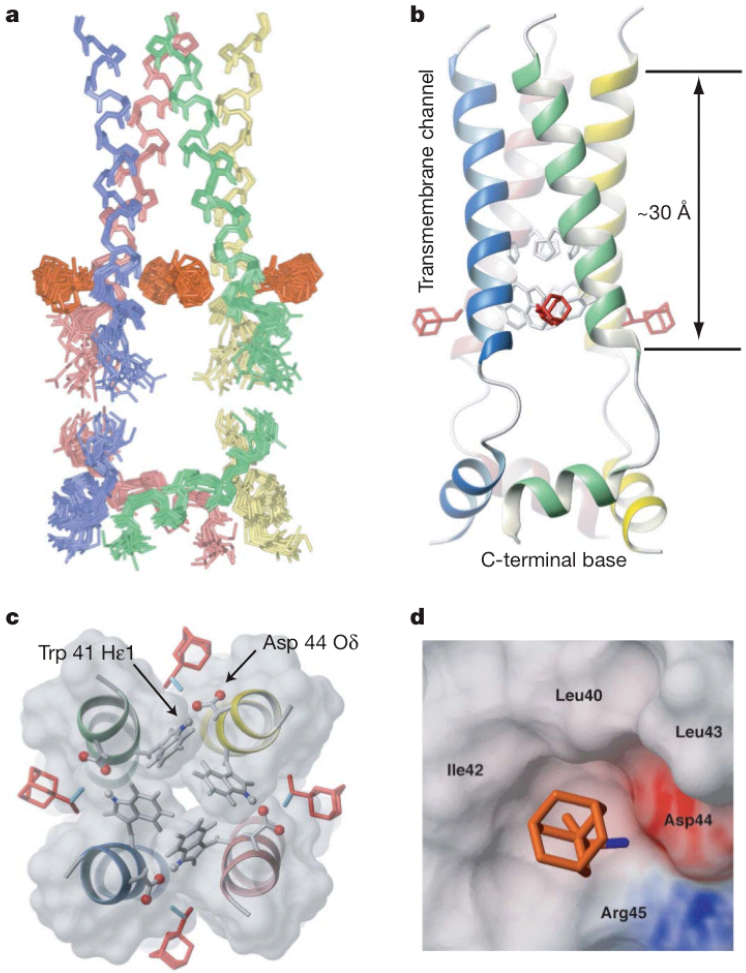

Figure 1 | Structure of the M2 channel. **a**, An ensemble of 15 low-energy structures derived from NMR restraints. Because residues 47–50 are unstructured, the transmembrane helices (residues 25–46) and the amphipathic helices (residues 51–59) are superimposed separately. The backbone r.m.s. deviations for the transmembrane and amphipathic helices are 0.30 Å and 0.56 Å, respectively. **b**, A ribbon representation of a typical structure from the ensemble in **a**, showing the left-handed packing of the transmembrane helices, right-handed packing of the amphipathic helices, the side chains of His 37 and Trp 41, and the drug rimantadine (coloured in red). **c**, A close-up view from the C-terminal side of the channel showing the Trp 41 gate and how it is stabilized by the inter-monomer hydrogen bond between Trp 41 Hε1 of one transmembrane helix and Asp 44 carboxyl of the adjacent transmembrane helix. **d**, The surface representation of the rimantadine-binding pocket, showing the Asp 44, the indole amine of Trp 41, and Arg 45, which form the polar patch, as well as the hydrophobic wall composed of Leu 40, Ile 42 and Leu 43.

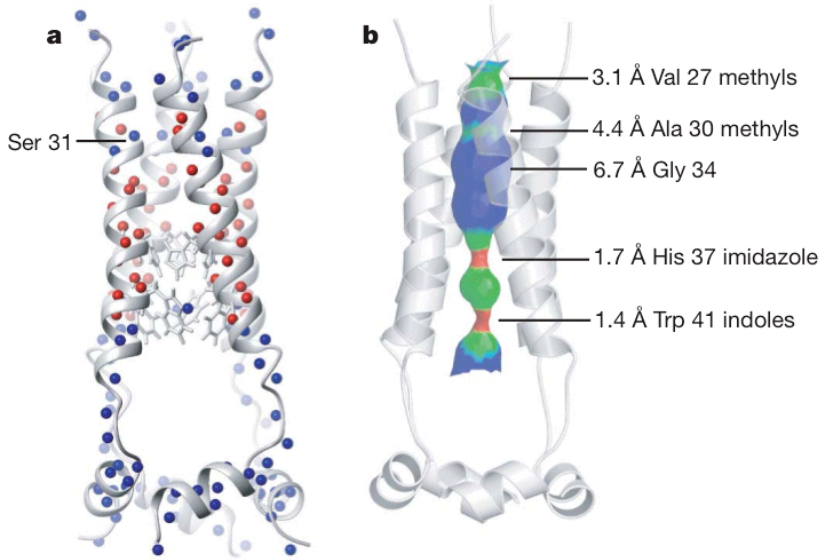

Figure 2 | Water accessibility of the M2 channel. **a**, Distribution of water NOEs relative to the structure. Amide protons coloured in blue have a NOE crosspeak to water. Those that do not are coloured red. **b**, The pore surface calculated using the program HOLE. The region of the channel coloured in green is only wide enough to allow passage of a water molecule, whereas the blue portion can accommodate two or more water molecules. The orange region is too narrow to allow any ions to pass through.

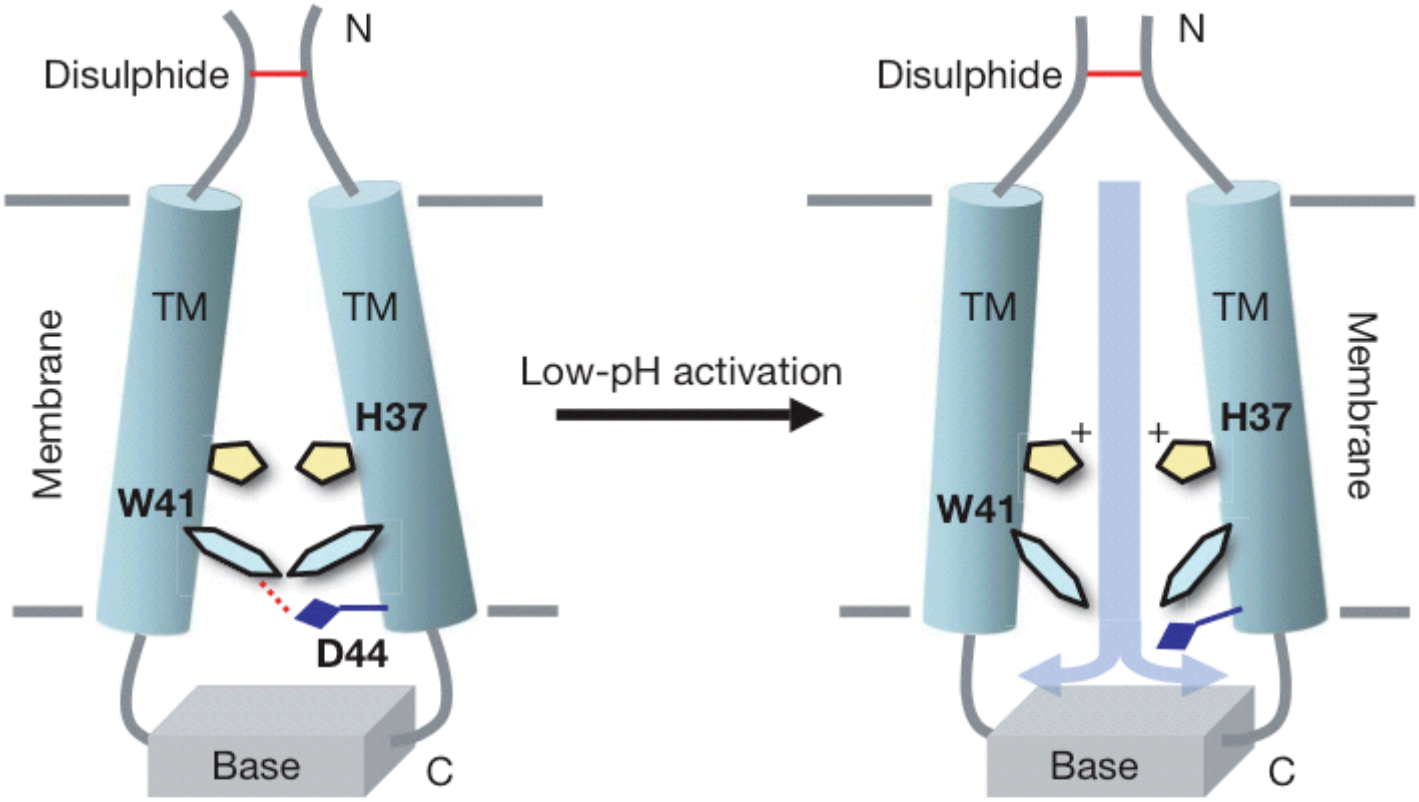

Figure 4 | Schematic illustration of M2 channel activation. At high pH, the transmembrane (TM) helices are packed tightly and the tryptophan gate is locked through intermolecular interactions with Asp 44. At low pH, protonation of the His 37 imidazoles destabilizes the transmembrane helix packing, allowing hydration of the channel pore and proton conductance. The C-terminal base of the tetramer and N-terminal disulphide bonds keep the channel from completely disassembling. For clarity, only two of the four monomers are shown.

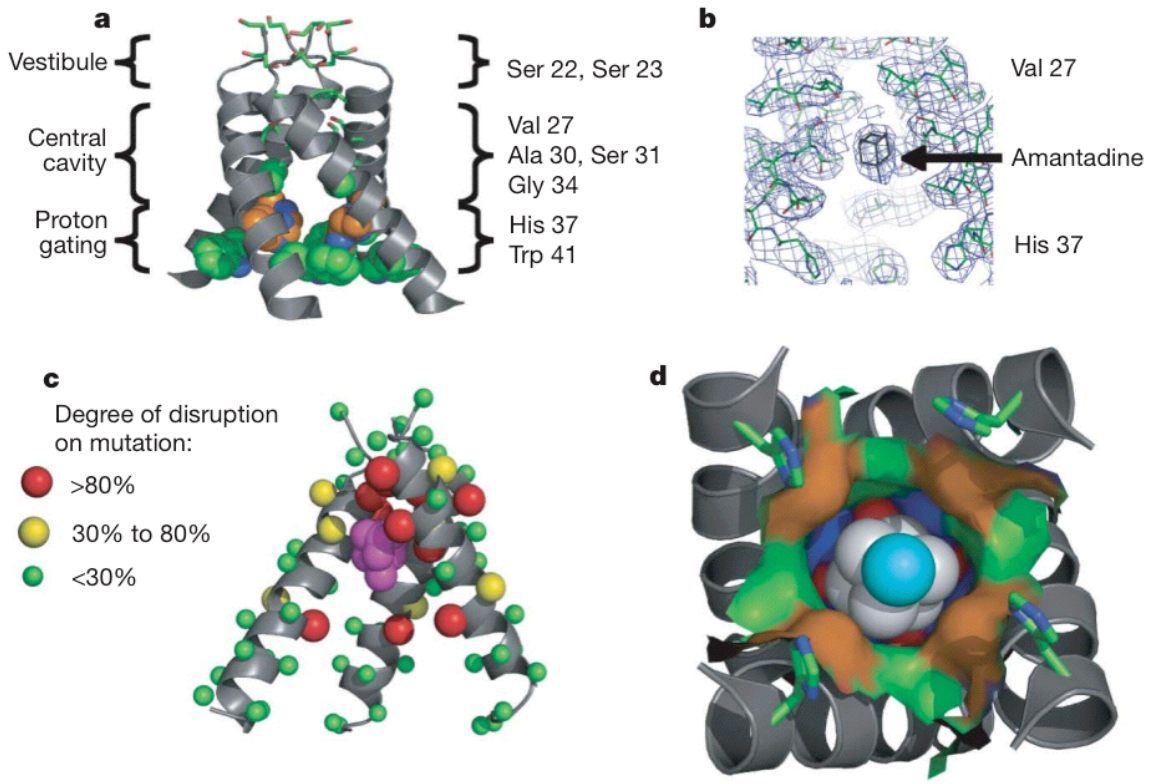

Figure 1 | Crystal structure of the M2 proton channel from the influenza A virus. **a**, The most critical residues identified by site-directed mutagenesis[5] line the pore. Gly 34, His 37 and Trp 41 are shown in space-filling spheres (carbon atoms of His 37 are coloured tan), whereas the side chains of the other critical residues are shown as sticks. **b**, Omit map ($2F_o - F_c$, contoured at 1σ) showing electron density in the amantadine-binding region. **c**, Positions of previously described Cys mutations[5] that disrupt the ability of amantadine to block the channel are shown by red balls (>80% disruption), yellow balls (30% to 80%) and green balls (no significant disruption) in full-length M2. Amantadine is shown in magenta. The front helix was removed for clarity. **d**, Structure of amantadine (nitrogen in cyan and carbon in white) inside the binding site showing the surface associated with residues Val 27 (red surface), Ala 30 (green), Ser 31 (blue) and Gly 34 (orange).

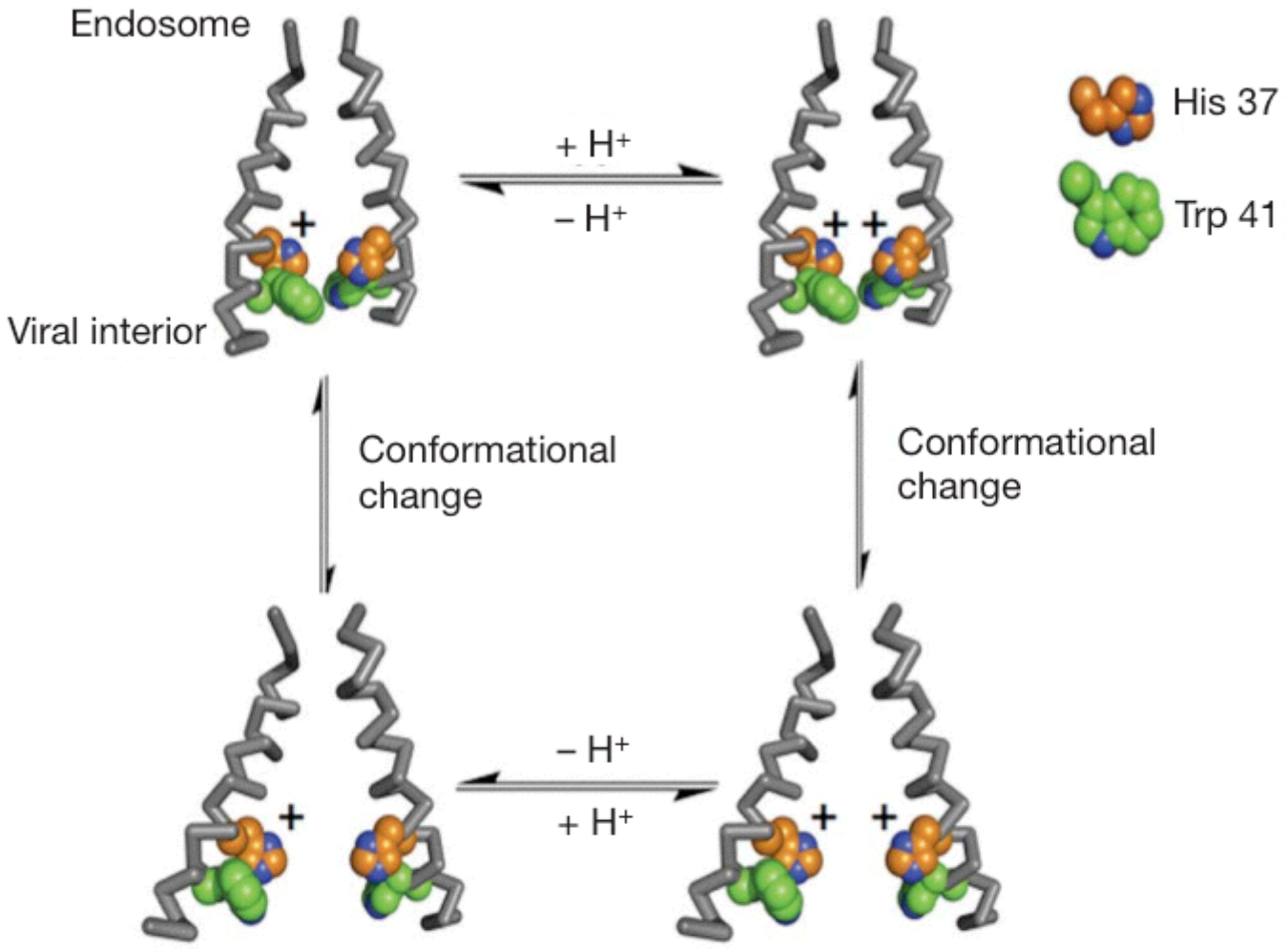

Figure 4 | Minimal mechanism of activation and conductance through the channel. Two helices of the tetramer and one protonation event are shown for simplicity.

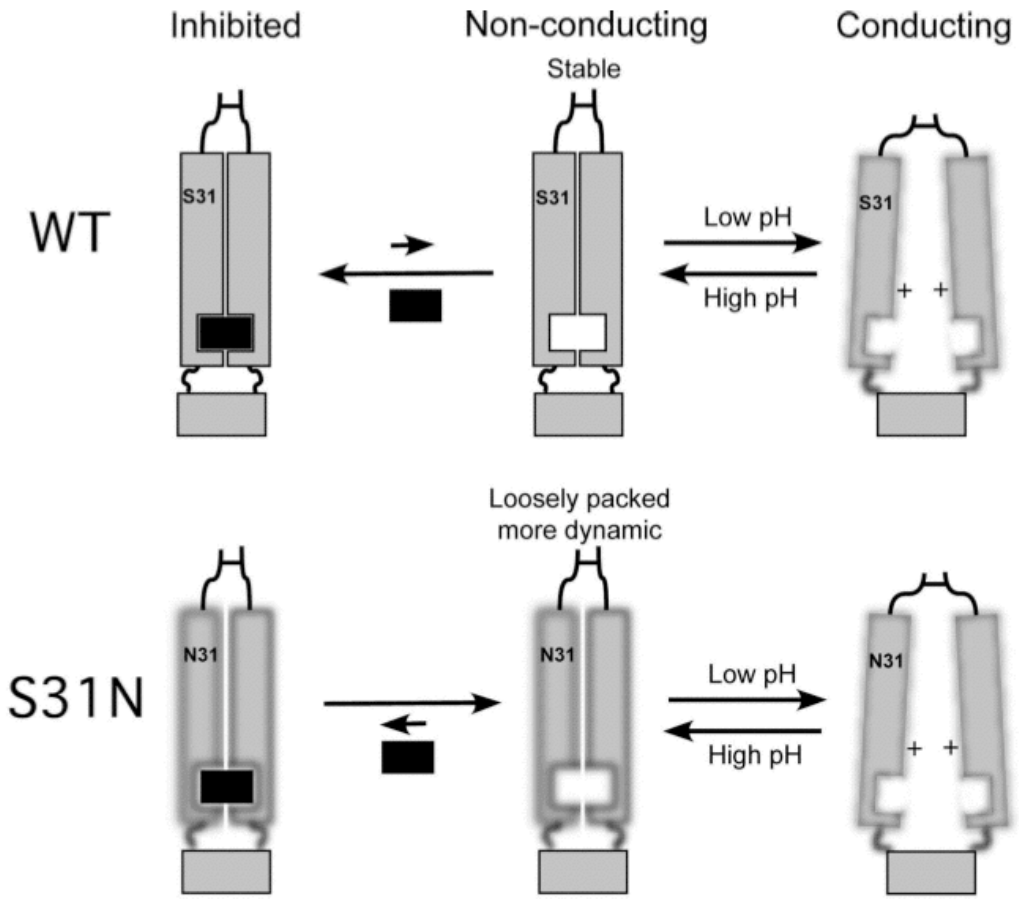

Fig. 6. Schematic representation of drug inhibition and drug resistance. In the WT channel, 2 adjacent TM helices form the lipid-facing pocket. The drug binds to the tightly assembled pocket in the closed state, making the channel harder to open. The S31N mutation weakens TM helical packing and thereby disrupts the drug pocket. Consequently, drug affinity is dramatically reduced while channel activity is preserved. The fuzzy lines represent increased conformational heterogeneity caused by weaker helical packing. Channel activation requires His-37 protonation at low pH; thus, destabilization of channel assembly is not sufficient for proton flux.

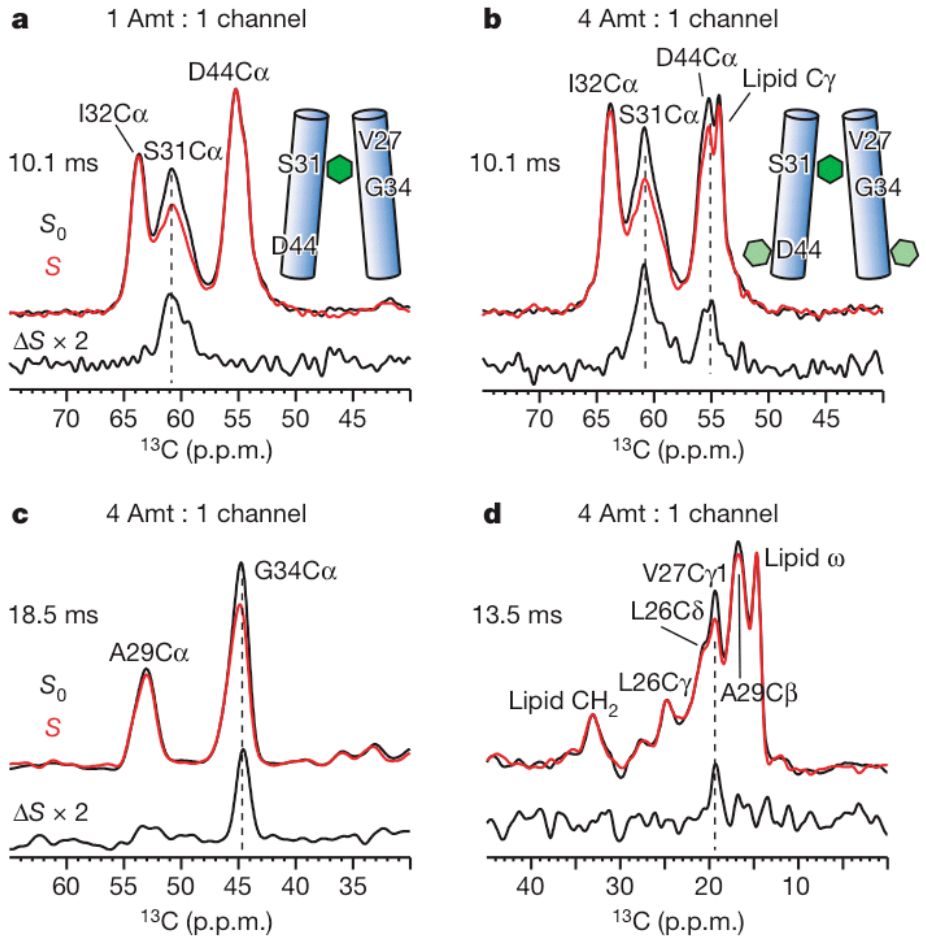

Figure 1 | Drug–protein proximities from $^{13}C\{^2H\}$ REDOR spectra of Amt-bound M2 in DMPC bilayers at two Amt/P ratios. Control (S_0), dephased (S, red) and difference (ΔS) spectra at specified mixing times are shown. **a**, Ser 31, Ile 32, Asp 44-labelled (SID) M2 at the stoichiometric ratio of Amt/P = 1:4. **b**, SID–M2 at the fourfold excess ratio of Amt/P = 4:4. Ser 31 Cα is dephased under both conditions but Asp 44 Cα is dephased only when Amt is in excess. **c**, **d**, Leu 26, Val 27, Ala 29, and Gly 34-labelled (LVAG) M2 at Amt/P = 4:4. **c**, Gly 34 Cα region. **d**, Val 27 Cγ1 region.

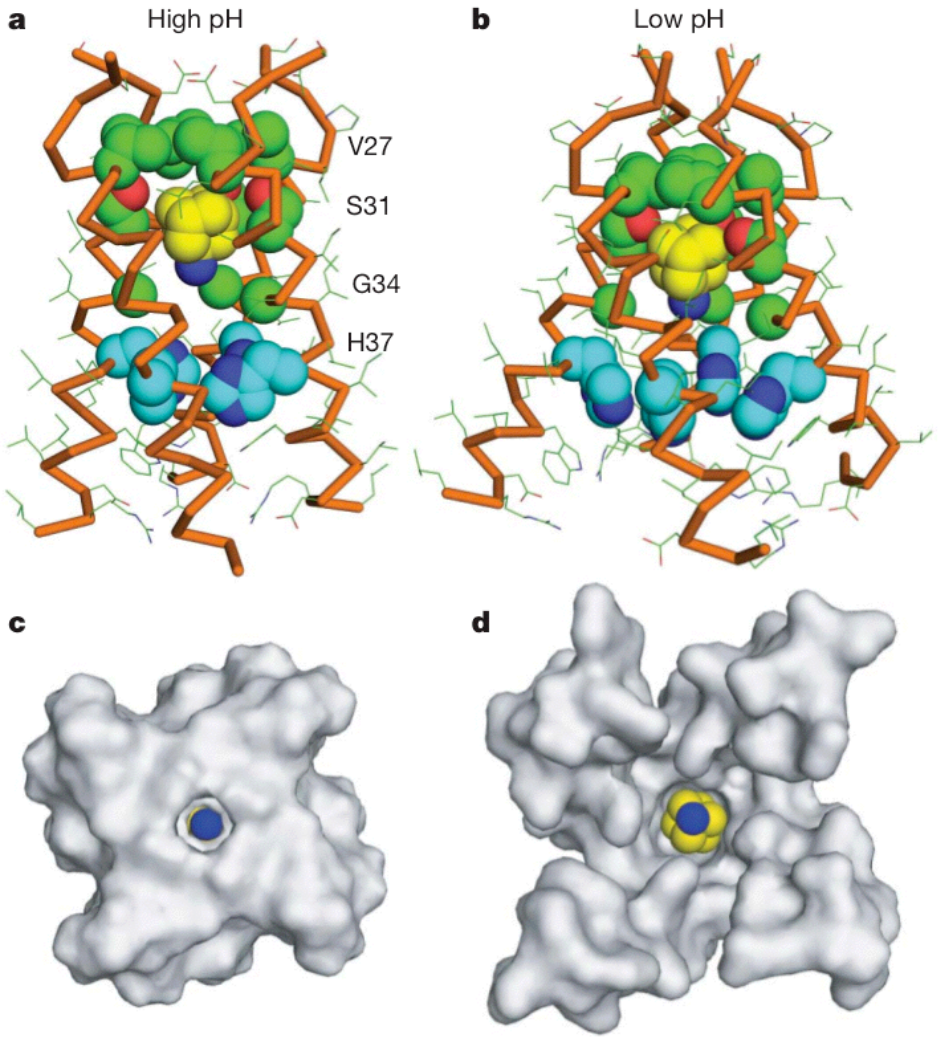

Figure 5 | Comparison of the high-pH SSNMR structure of Amt-bound M2 in lipid bilayers with the low-pH crystal structure of Amt-bound M2. **a**, Side view of the high-pH SSNMR structure, showing Amt to be enclosed by Val 27 at the top and His 37 at the bottom. **b**, Side view of the low-pH crystal structure[2]. The helices are splayed far apart near the C terminus. **c**, C-terminal view of the high-pH structure, showing a well-sequestered drug. **d**, C-terminal view of the low-pH structure, showing a more solvent-accessible drug. The figure was generated using the program PyMOL.